

Sensitivity Analysis of a Thermo-Structural Model for Materials in Fire

PATRICK SUMMERS, BRIAN LATTIMER, SCOTT CASE, and STEPHANIE FEIH

Department of Mechanical Engineering

Virginia Tech

110 Randolph Hall, Blacksburg, VA 24061, USA

ABSTRACT

A new thermo-structural model was developed and validated to predict the failure of compressively loaded fiber-reinforced polymer (FRP) laminates during one-sided heating from a fire. The model consists of the best thermal and structural models in the literature integrated into a single predictive model. This includes a one-dimensional pyrolysis model to predict the thermal response of a decomposing material. Using the thermal response to calculate the mechanical properties, an integral structural model was developed considering thermally-induced bending caused by one-sided heating. The thermo-structural model predicts out-of-plane deflections and compressive failure of laminates in fire conditions. This paper also provides an improved failure model for FRP laminates exposed to fire, a first validation study on the modeling approach using intermediate-scale compression load failure tests with a one-side heat flux exposure, and a first sensitivity study of the input parameter effects on the structural response of FRP laminates. Through the sensitivity study, the out-of-plane deflection predictions exhibited little sensitivity to the thermal inputs. However, the time-to-failure predictions were significantly affected by the virgin conductivity and specific heat capacity. The structural inputs exhibited a significant impact on the out-of-plane deflection predictions. The in-plane thermal expansion, residual elastic modulus above the glass transition temperature, and vertical temperature profile significantly affected the magnitude of the out-of-plane deflection; however, only the in-plane thermal expansion and residual elastic modulus affected the failure direction. The time-to-failure prediction was only significantly affected by the residual elastic modulus. A better agreement between the predicted and observed times-to-failure was achieved by reducing the residual elastic modulus.

KEYWORDS: sensitivity, thermo-structural, modeling, composites, FRP laminate.

NOMENCLATURE LISTING

A	cross-sectional area (m^2)	T_k	glass transition temperature ($^{\circ}\text{C}$)
C	specific heat capacity (J/kg)	T_{ref}	reference temperature (0°C)
e	eccentricity (m)	v	out-of-plane deflection (m)
E	elastic modulus (Pa)	x	axial direction (m)
E_a	activation energy (J/gmol)	y	through-thickness direction (m)
I	moment of inertia (m^4)	Greek	
k	conductivity ($\text{W/m}\cdot^{\circ}\text{C}$)	α	in-plane thermal expansion ($1/^{\circ}\text{C}$)
K	vertical temperature fitting parameter	ε	strain (m/m)
l	thickness (m)	Φ	thermal softening parameter
L	effective bending length (m)	ρ	density (kg/m^3)
\dot{m}_g	mass flux of pyrolysis gases ($\text{kg/m}^2\cdot\text{s}$)	σ	stress (Pa)
M	bending moment ($\text{N}\cdot\text{m}$)	θ	slope (rad)
n	order of reaction	subscripts	
P	axial load (N)	d	decomposed
Q	heat of decomposition (J/kg)	g	gases
R	universal gas constant ($\text{J/gmol}\cdot\text{K}$)	m	mechanical
t	time (s)	v	virgin
T	temperature ($^{\circ}\text{C}$)	T	thermal

INTRODUCTION

Fiber-reinforced polymer (FRP) laminates have seen an increase in interest for use in naval applications due to its low weight and high corrosion resistance when compared to traditional construction materials

such as steel. As a result, FRP laminates are under consideration for use in entire load-bearing structures. However, the laminates are combustible materials that decompose and burn when exposed to a sufficiently strong heat source, such as that present in fire conditions. Additionally, the mechanical properties of FRP laminates decrease significantly as the material temperature increases above the glass transition temperature (approximately 120 °C for the vinyl ester resin being considered for naval applications) [1]. As a result, a major design challenge for use of FRP laminates is fire performance.

The fire performance of FRP laminate naval structures may be evaluated either through large-scale testing or computational modeling. The more traditional method is to conduct large-scale testing. While large-scale tests provide the most representative data that may be obtained for a given structure, they are expensive and time consuming. The high cost in terms of both time and money involved in running such tests renders parametric studies for design optimization highly impractical. In order to reduce the number of tests required, tests performed at a smaller scale and computational models may be used to conduct parametric studies and design optimizations, saving large-scale tests for validation at the end of the design process. Thermo-structural modeling of fire-exposed laminates is less expensive than large-scale tests and provides the opportunity to perform parametric studies to support design optimization. Thermo-structural modeling of FRP laminates requires a coupled thermal and structural model. A pyrolysis model capable of capturing laminate decomposition during heating should be used to predict the thermal response. Using the thermal response predictions, predictions can be performed on the degradation of mechanical properties of the laminate. The predicted mechanical properties may be applied in a variety of structural models to predict the laminate's response to compressive loading conditions.

Numerous studies have been performed developing pyrolysis models to predict the thermal response of FRP laminates in fire. Henderson et al. [2,3] adapted pyrolysis models first developed for wood for use with FRP laminates. Numerous one-dimensional pyrolysis models for FRP laminates have since been developed based upon those developed by Henderson, et al. [4–7]. Enhancements to these models were presented in subsequent studies by extending thermal predictions into multiple dimensions and adding additional material behaviors [8–11]. Gibson et al. [12] and Feih et al. [13,14] developed semi-empirical mechanical property degradation models which capture the temperature and decomposition-state dependence of the material.

Numerous models exist to predict the thermo-structural response of compressively loaded FRP laminates in fire conditions. These models range in complexity from simply implemented analytical solutions to finite element simulations. They also differ in implementation of the thermal portion of the model, mainly through the use of either a pyrolysis model or an assumption of the thermal response of the laminate. A thermo-structural model was developed by Asaro and colleagues [15,16] which used a simple heat conduction model and beam theory to predict the structural response of a thermally-exposed laminate. Liu et al. [17] developed a model assuming a linear temperature gradient based on steady-state conduction. The structural model included thermal effects by use of a thermal moment caused by non-uniform mechanical properties. Kardomateas and colleagues [18,19] advanced this model through implementation of a heat conduction model with material decomposition as a function of exposure time; however, the mechanical properties were coarsely approximated and do not capture the effects of decomposition until decomposition is 80 % complete. Feih et al. [13,14] developed a model that evaluates the compressive failure of FRP laminates using bulk analysis. The bulk compressive strength was compared with the applied stress to predict laminate failure.

A new model is developed in this paper to predict failure of compressively loaded FRP laminates that combines the best thermal and structural models from previous work into a single predictive model. The thermal model was developed based on the one-dimensional pyrolysis models developed by Henderson et al. [2] and Lattimer et al. [20]. Mechanical properties were calculated using the predicted temperatures and material decomposition state using the model developed by Gibson et al. [12]. The methodology developed by Liu et al. [17] was implemented to predict the structural response with inclusion of temperature and decomposition state dependent mechanical properties. The principles used by Feih et al. [13,14] to predict failure based on compressive strength were modified to predict failure. The compressive strength was calculated through the laminate thickness using the model developed by Gibson et al. [12]. A localized failure criterion was used where failure is predicted when the maximum combined compressive stress exceeds the compressive strength at any point through the laminate thickness. The research also expanded on the state-of-the-art by implementing an improved failure model, performing the first validation of the

modeling approach with intermediate-scale compression load failure tests with one-sided heat exposure, and conducting the first sensitivity study of the input parameters on the structural response of FRP exposed to fire with compressive loading.

MATHEMATICAL FORMULATION

A thermo-structural model was developed to predict the failure of compressively loaded FRP laminates exposed to non-uniform, one-sided heating. The thermal model was developed as a one-dimensional pyrolysis model which predicted the temperature and decomposition response for a decomposing material. The structural model represented the behavior of the compressively loaded laminate as a beam. The thermal model is integrated with the structural model to predict the change in mechanical properties. An analytical solution is obtained for the structural response of the beam with a case of non-uniform, one-sided heating of the laminate. Out-of-plane deflections and maximum combined compressive stress due to axial compression and bending were calculated and compared to the compressive strength to determine failure.

Thermal Model Development

A pyrolysis model was developed to predict the thermal response of FRP laminates subjected to fire conditions, specifically one-sided heating. The physical behavior of a decomposing laminate subjected to one-sided heating is shown in Fig. 1. As heat is applied to the laminate, the material will reach a temperature where the solid is converted into a gas. The decomposition of the virgin (solid) material occurs at the pyrolysis front and results in the formation of char and pyrolysis gases. After decomposition is complete, the remaining material is a fiber/char matrix. The pyrolysis gases are transported toward the heated surface of the laminate through the fiber/char region. The pyrolysis gas transport within the laminate causes internal convection, cooling the material as it flows to the surface. This is an important effect that must be taken into account to accurately predict the thermal response of a decomposing material.

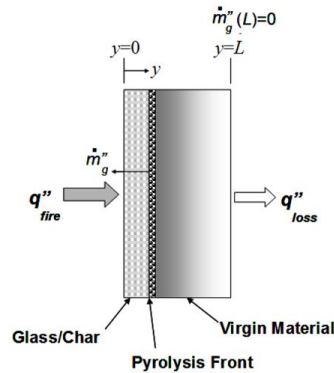


Fig. 1. Decomposition of an FRP laminate exposed to one-sided heating.

The behavior of the thermal response is governed by three equations: the energy equation, solid material decomposition model, and conservation of mass equation. The one-dimensional energy equation in Eq. 1 was obtained assuming constant, uniform heating, insulated edges, and constant volume.

$$\rho C \frac{\partial T}{\partial t} + (h - h_g) \frac{\partial \rho}{\partial t} + \dot{m}_g C_g \frac{\partial T}{\partial y} = \frac{\partial}{\partial y} \left(k \frac{\partial T}{\partial y} \right) \quad (1)$$

The enthalpies were defined as

$$h = Q + \int_{T_{ref}}^T C dT, \quad h_g = \int_{T_{ref}}^T C_g dT \quad (2)$$

The heat of decomposition, Q , is defined as negative for an endothermic process. The thermal properties, k , C , and C_g , are defined as dependent on both temperature and decomposition state. The first term in Eq. 1 represents the time-temperature response of the material. The second term represents the energy required to

decompose the solid material. The third term represents the internal convection due to the flow of pyrolysis gases. The term on the right hand side represents heat conduction through the material thickness.

The solid material decomposition model calculates the change in density with time. The approach chosen for the decomposition model was an n^{th} order Arrhenius kinetics equation

$$\frac{\partial \rho}{\partial t} = -(\rho_v - \rho_d) \left[\frac{\rho - \rho_d}{\rho_v - \rho_d} \right]^n A \exp\left(\frac{-E_a}{RT}\right) \quad (3)$$

This expression is advantageous for use in modeling because it scales the results based on the fraction of material involved in the decomposition process (active material). Therefore, results are scaled from zero to unity based on the relative decomposed state of the material.

The conservation of mass equation is used to determine the mass flux of pyrolysis gases. At the heated surface, the mass flux of pyrolysis gases is equal to the mass loss rate of the material. Assuming constant volume and that the mass of solid material is much greater than that of pyrolysis gases, the conservation of mass equation reduces to

$$\frac{\partial \dot{m}_g}{\partial y} \delta y = -\frac{\partial \rho}{\partial t} \quad (4)$$

The mass loss rate may be determined at any point within the material by integrating the expression from a location within the material (y') to the unheated surface (l). Assuming instantaneous flow of the pyrolysis gases to the heated surface and zero mass flux at the unheated surface, the equation is reduced to

$$\dot{m}_g(y', t) = \int_{y'}^l \frac{\partial \rho}{\partial t} \quad (5)$$

where the change in density with time is solved directly as a function of time using the solid material decomposition model in Eq. 3.

The fire behavior of timber structures is typically characterized using a definition of the charring rate for a given material. This concept may be applied to FRP laminates, though, as for timber, the heat flux and convective conditions will affect the charring rate [21]. Mouritz and Mathys [22] determined that the rate of growth of the char layer thickness is non-constant over time and is dependent on both the exposure time and applied heat flux for FRP laminates. It is important to also note that the laminate decomposes from a solid to a gas over a range of temperatures. The decomposition begins as low as approximately 140 °C with the majority of decomposition occurring over the range of approximately 380 °C to 480 °C. The temperature at the onset of decomposition will also be lower (380 °C) for lower heating rates (5 °C/min) and higher (420 °C) for higher heating rates (40 °C/min) [23].

The boundary conditions considered in the thermal model are defined temperature, defined heat flux, or a combined boundary condition considering heat flux, convection, and radiation. The combined boundary condition best fits the case of one-sided heating considered in fire conditions. The thermal model initial conditions are defined for the temperature and density. The initial material temperature is defined through the material thickness. The initial material density is defined as the virgin density.

Thermal model validation was performed using an E-glass vinyl ester FRP composite heated in a cylindrical ceramic heater. A detailed description of the experimental apparatus, experiment, and material thermal properties is available in Lattimer et al. [20]. The E-glass vinyl ester sample was manufactured using a quasi-isotropic layup with a brominated Derakane 510A resin. The sample was 12.7 mm thick with exposed dimensions of 100 mm by 100 mm. A 38.1 mm thick piece of ceramic insulation board was attached to the unexposed surface of the sample. A shutter was used to allow preheating of the heater; however, this caused a slight ramping of the applied heat flux at test initiation. The heat flux was measured using a 0–200kW/m² Schmidt-Boelter type total heat flux gauge. The mass loss rate of the sample was

measured using a load cell. The measured change in mass was divided by the cross-sectional area of the sample to determine mass flux. Temperatures were measured using thermocouples at the exposed surface, mid-depth, and interfacial surface between the sample and insulation board.

The results of the thermal model validation are shown in Fig. 2. The predicted temperatures compare well against experimental temperatures. The virgin and decomposed conductivity for the given material system are

$$k_v = (4.405 \times 10^{-5})T + 0.312 \quad k_d = (2.83 \times 10^{-4})T + 0.0949 \quad (6)$$

The predicted mass flux at the exposed surface compares well against the experimental data. The predicted mass flux has a noticeable spike at test initiation. This is attributed to the solid material decomposition model using a single-step global reaction mechanism. In reality, the FRP laminate decomposition includes multiple reactions and the failure to represent all of these reactions may explain the behavior of the model at test initiation.

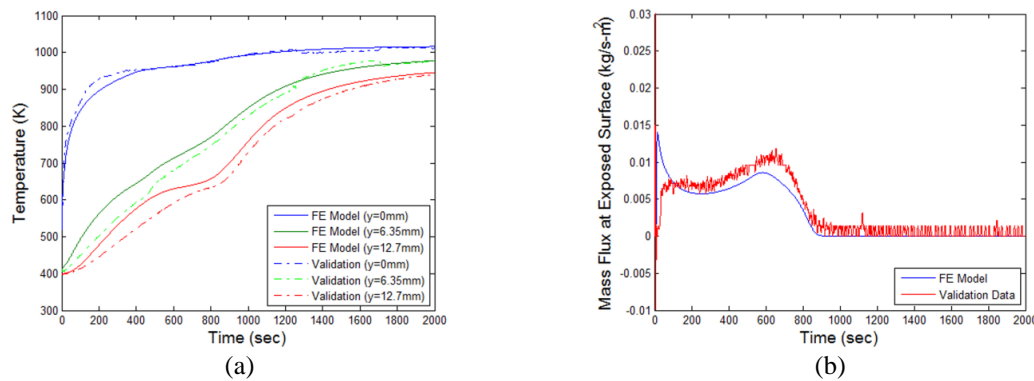


Fig. 2. Thermal model validation with: (a) temperatures; (b) mass flux at the exposed surface compared against experimental data.

Thermo-Structural Model Development

The thermo-structural model was developed to predict the structural response of a decomposing laminate subjected to an axial, compressive load in fire conditions. The structural response of a decomposing laminate is closely linked to its thermal response, which is predicted using the thermal model.

Consider an FRP laminate fixed at both ends and compressively loaded. The compressive load is applied at the centerline of the laminate, which is initially coincident with the neutral axis. The structural response in this case is governed by Euler buckling. A heat source is applied to one side of the laminate, causing a parabolic vertical temperature profile. The mechanical properties of the laminate are temperature dependent; therefore, the temperature gradient non-uniformly degrades the mechanical properties through the thickness. This causes the neutral axis to shift away from the centerline resulting in eccentric loading and moments developing at the fixed ends of the laminate. The equivalent moment loading is shown in Fig. 3a. Additionally, the temperature gradient will cause non-uniform in-plane thermal expansion through the thickness. This causes a moment to develop at the fixed ends due to non-uniform reaction forces from thermal expansion. This moment is referred to as the thermal moment.

The out-of-plane bending of the laminate will change the governing mechanics from Euler buckling to bending. The laminate essentially behaves as an axially compressed beam experiencing bending due to moments at the fixed ends as depicted in Fig. 3c. To model the structural response, the thermo-structural model is divided into two distinct parts. The thermal model predicts the temperature gradient and decomposition state of the laminate at the mid-height. The structural model calculates the mechanical properties as a function of temperature and decomposition state. The thermal moment and shift in neutral axis (eccentricity) are then calculated and scaled with height based on the vertical heat distribution. The analytical solution derived for a laminate with fixed end conditions uses these mechanical properties to calculate the out-of-plane deflection and maximum combined compressive stress in the laminate.

Several key assumptions were made to simplify the behavior of a compressively loaded, heated laminate. The first assumption is that the non-uniform, one-sided heating produces a parabolic temperature profile along the laminate height. This extends the thermal model predictions of the mid-height through-thickness temperatures two-dimensionally along the length of the laminate. This assumption is used in the structural model for the thermal moment and eccentricity, which are also assumed to follow this parabolic shape. The remaining assumptions are the axial movement of the laminate is unrestrained and the laminate experiences only small deflections prior to failure.

The governing equation was developed for the case of an axially compressed laminate with fixed end conditions and centered, non-uniform heating. Performing a moment balance about the origin of the coordinate axes in Fig. 3a

$$\sum M_O = M(x) + Pe(x) + Pv(x) = 0 \quad (7)$$

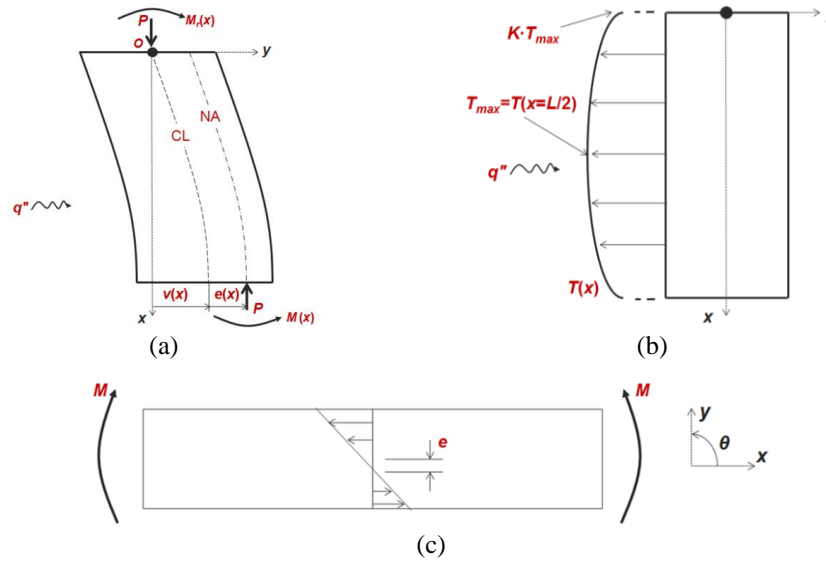


Fig. 3. Laminate showing: (a) eccentric loading and bending moment; (b) vertical temperature profile along exposed surface; (c) bending moment with eccentricity.

The bending moment, $M(x)$, is a result of the beam curvature and non-uniform, in-plane thermal expansion. Consider the unheated beam in Fig. 3c to define the relation between the moment and curvature. The beam curvature is related to the strain and derivative of the slope as follows

$$\varepsilon = \frac{-(y-e)}{\kappa} = -(y-e) \frac{d\theta}{dx} \quad (8)$$

The bending moment is calculated in relation to stress using the one-dimensional stress-strain relationship including the thermal strain due to in-plane thermal expansion.

$$M = -\int \sigma(y-e) dA = -\int E(\varepsilon - \varepsilon_T)(y-e) dA \quad (9)$$

where the eccentricity is included to account for the shift in neutral axis. The total strain in Eq. 8 and the thermal strain, defined as the in-plane thermal expansion, are substituted into the above equation

$$M = \frac{d\theta}{dx} \int E(y-e)^2 dA + \int E\alpha\Delta T(y-e) dA \quad (10)$$

where the equivalent bending rigidity, $(EI)_{eq}$, is defined as the first integral term and the thermal moment, M_x^T , is defined as the second integral term. Substituting for the bending moment in Eq. 7, taking the derivative with respect to the axial direction, x , and applying a small angle assumption results in

$$(EI)_{eq} \frac{d^2\theta(x)}{dx^2} + P\theta(x) = -\frac{dM_x^T(x)}{dx} - P \frac{de(x)}{dx} \quad (11)$$

The relationships for the eccentricity and thermal moment were developed using the assumption of a parabolic shape of the heat source with height, depicted in Fig. 3b. Criteria were placed on the parabolic shape such that it must be at a maximum at the mid-height ($x = L/2$) and reduce to a percentage of the maximum value at the ends of the laminate ($x = 0, L$). The parabolic shape functions were defined as

$$e(x) = e_0 \left[-\left(4 - 4K\right) \left(\frac{x}{L}\right)^2 + \left(4 - 4K\right) \left(\frac{x}{L}\right) + K \right] \quad (12)$$

$$M_x^T(x) = M_{x,0}^T \left[-\left(4 - 4K\right) \left(\frac{x}{L}\right)^2 + \left(4 - 4K\right) \left(\frac{x}{L}\right) + K \right] \quad (13)$$

where the vertical temperature profile fitting parameter, K , is a scaling parameter which scales the temperatures at the fixed ends of laminate based on those at the mid-height. Taking the derivative of these equations and substituting into Eq. 11 results in

$$(EI)_{eq} \frac{d^2\theta(x)}{dx^2} + P\theta(x) = \left(M_{x,0}^T + Pe_0 \right) \left(\frac{8-8K}{L^2} x - \frac{4-4K}{L} \right) \quad (14)$$

This is the final form of the governing equation used to develop the analytical solution. Enforcing the boundary conditions for fixed-fixed end conditions, the slope is solved for as a function of beam height. Integrating the solution for the slope to obtain the out-of-plane deflections as a function of beam height results in

$$v(x) = \frac{4-4K}{L} \left(\frac{M_{x,0}^T}{P} + e_0 \right) \left(\frac{\cos(\lambda_c L) + 1}{\lambda_c \sin(\lambda_c L)} (\cos(\lambda_c x) - 1) + \frac{\sin(\lambda_c x)}{\lambda_c} + \frac{x^2}{L} - x \right) \quad (15)$$

where λ_c is developed from the governing equation in Eq. 11

$$\lambda_c = \sqrt{\frac{P}{(EI)_{eq,av}}} \quad (16)$$

The bulk equivalent bending rigidity of the laminate, $(EI)_{eq,av}$, is calculated as a bulk value through the thickness.

The mechanical property relationships for the elastic modulus and compressive strength were implemented as the semi-empirical relationship developed by Gibson et al. [12] and Feih et al. [13,14]. The semi-empirical relationship for the mechanical properties as a function of temperature and decomposition state is

$$E(T) = \left(\frac{E_{(0)} + E_{(R)}}{2} - \frac{E_{(0)} + E_{(R)}}{2} \tanh(\Phi(T - T_k)) \right) R_{rc}(T)^\beta \quad (17)$$

where the elastic modulus, E , may also be replaced by the compressive strength, σ_c to provide the variation in compressive strength with temperature. The reduction of the mechanical properties due to decomposition is taken into account using the scaling function, R_{rc} . This function is the instantaneous mass fraction, F , as calculated by the thermal model. A fitting parameter, β , was used to fit the scaling function to measured data.

Non-uniform through-thickness temperatures cause a non-uniform elastic modulus through the thickness. This shifts the neutral axis from the mid-surface and this distance (eccentricity) is calculated as

$$e = \frac{\int_A E(T)y dA}{\int_A E(T) dA} \quad (18)$$

The maximum stress developed in the laminate due to axial compression and bending is calculated using superposition of strains. The mechanical strain within the laminate is calculated by superimposing the axial and bending strains. Applying the stress-strain relationship, $\sigma = E\varepsilon_m$, results in the combined compressive stress

$$\sigma(x) = -\frac{P}{A} - E(y - e)\frac{d\theta(x)}{dx} - E\alpha\Delta T \quad (19)$$

where the maximum combined compressive stress for the selected case will occur at the laminate mid-height, $x = L/2$. This is apparent in the development of the governing equation where the vertical temperature profile and, therefore, eccentricity and thermal moment are at a maximum at the mid-height. Also, the maximum out-of-plane deflection occurs at the mid-height for a beam with symmetric end conditions.

The thermo-structural model uses a localized failure criterion to determine laminate failure. Failure is predicted when the maximum combined compressive stress is equal to the compressive strength at the same location. The model does not include progressive failure; therefore, when failure is predicted at a single point within the laminate, the laminate is assumed to fail. The time-to-failure is defined as the time elapsed prior to failure.

Thermo-Structural Model Implementation

The structural model developed for a compressively loaded, heated FRP laminate was integrated with the thermal model, forming the thermo-structural model. Essentially, the structural model is used as a post-processing step to the thermal model using the thermal predictions as inputs to calculate the mechanical properties. The out-of-plane deflection and maximum combined compressive stress is then calculated using the analytical solution. The laminate is determined to fail when the maximum combined stress exceeds the compressive strength.

The mechanical properties are calculated at the nodes using the predicted temperatures and decomposition state. Bulk mechanical properties, such as the bulk equivalent bending rigidity, were calculated using Simpson's integration technique where the number of intervals is identical to the number of elements in the thermal model. The eccentricity and thermal moment were calculated in a similar manner. The mechanical properties were used to calculate the eccentricity and thermal moment at each node. Simpson's integration technique was then applied to obtain the eccentricity and thermal moment for use in the analytical solution.

THERMO-STRUCTURAL MODEL VALIDATION AND SENSITIVITY

The thermo-structural model was validated using one-sided heating tests performed on compressively loaded, intermediate-scale (737 mm bending length and 203 mm width) E-glass vinyl ester laminates. The flat-plate geometry and intermediate sized laminates were chosen to simplify the thermo-structural analysis and aid in development and understanding of modeling techniques. Structural features, such as hat stiffeners, and insulation which would be used in the large-scale application of FRP laminates to improve fire resistance were not included in order to simplify the analysis.

Laminates were exposed to a constant heat flux produced using an electrical radiant heater bank 910 mm high and 300 mm wide. Refer to Summers [24] for details. The thermo-structural modeling of the intermediate-scale tests used the thermal and mechanical properties of E-glass Derakane 411-350 vinyl ester laminates [24]. The model was first validated using the intermediate-scale tests. The sensitivity of the out-of-plane deflection and time-to-failure predictions to the thermo-structural model inputs was then analyzed to determine the possible causes of differences between predictions and test observations.

Comparison of Model Predictions to Test Results

One test was selected to demonstrate the predictive capabilities of the thermo-structural model, additional comparisons for all intermediate-scale tests performed are available in Summers [24]. The test selected was performed on a laminate with a 12 mm thickness, a 38 kW/m^2 heat flux, and an applied load of 25 % of the Euler buckling load. Plots of the model validation are shown in Fig. 4. In these plots, the lines and symbols represent model predictions and test data, respectively. The mid-height through-thickness temperature profile and out-of-plane deflection comparisons are shown. Deflections are defined as positive towards the heat source. The local failure criterion is plotted as the maximum combined compressive stress normalized by the compressive strength. Laminate failure is predicted when the normalized maximum stress exceeds the compressive strength, which is represented by the solid line at unity.

The model predictions for the through-thickness temperatures in Fig. 4c compare with the test data except for the measurements within the thickness of the laminate, specifically at the 4mm depth. This deviation may be associated with the thermocouple attachment technique. The error associated with the hole depth for the thermocouple causes an error associated with the temperature measurement depth. However, the predicted temperatures fall within the error bounds for the possible measurement error associated with thermocouple depth. The predicted time-to-failure agrees well with that observed in the test. However, the predicted out-of-plane deflection in Fig. 4a does not agree well with that observed in the test. The difference between the predicted and observed out-of-plane deflection may be due to incorrect model inputs. This sensitivity of the deflection prediction to model inputs was a major motivation for performing the sensitivity analysis.

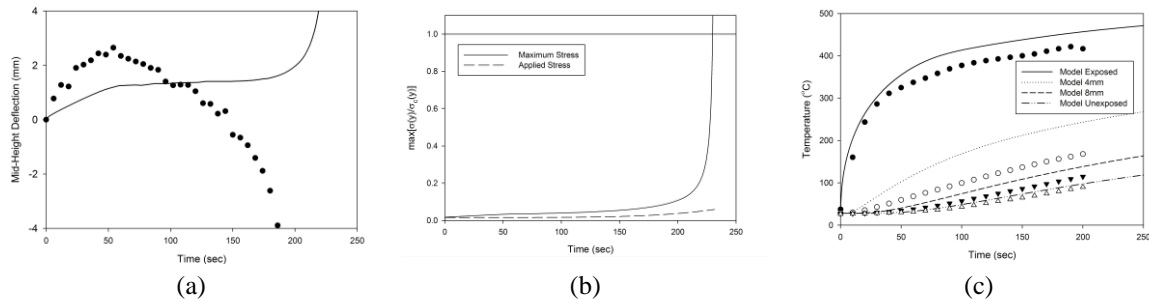


Fig. 4. Comparison of the thermo-structural model predictions to the intermediate-scale test results for 12 mm, 38 kW/m^2 , 25 % buckling load test. Predicted time-to-failure was 232 s and experimental time-to-failure was 193 s.

The time-to-failure predictions for the intermediate-scale tests were compared against the observed times-to-failure in Fig. 5. The plot in Fig. 5a shows good agreement between the predicted and observed times-to-failure. Two tests at 25 % of the buckling load and 8 and 12 kW/m^2 heat fluxes were not predicted to fail. The outliers for the shorter failure times correspond to tests performed at loads exceeding 50 % of the buckling load for the 9 mm and 6 mm thicknesses.

Sensitivity of Model Predictions

A study was performed to determine the sensitivity of the thermo-structural model predictions to the thermal and mechanical material properties. The specific output parameters investigated were the predicted mid-height out-of-plane deflection and time-to-failure. The thermal material properties that were investigated are those contained in the energy equation in the thermal model. These properties are the virgin (k_v , C_v), decomposed (k_d , C_d), and bulk conductivity (k) and specific heat capacity (C) and also the enthalpy (h) and enthalpy of gases (h_g). The mechanical material properties are those contained in the

analytical solution and the mechanical property degradation model for the elastic modulus in the structural model. These properties are the in-plane thermal expansion (α), the residual elastic modulus ($E_{(R)}$), and the vertical temperature profile fitting parameter (K). The sensitivity of the model outputs was determined using tests performed on a 12mm thick laminate with a 38 kW/m² heat flux and applied loads of 15 %, 25 %, and 50 % of the Euler buckling load. The sensitivity to the structural model inputs was determined using all three cases; however, the thermal model sensitivities were determined only using the 25 % applied load case.

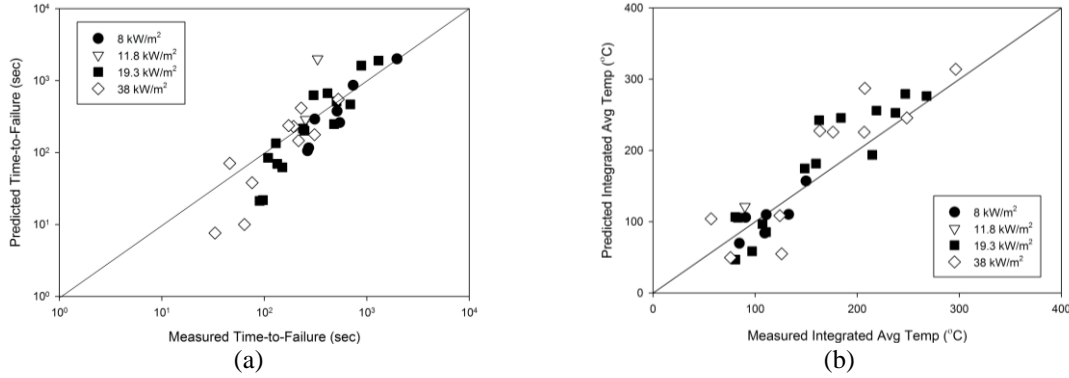


Fig. 5. Plots of the predicted and observed: (a) times-to-failure; (b) average temperatures at failure.

The sensitivity analysis for thermal properties was performed by varying the input parameters individually from 50 to 150 % of their original value. The results of the thermal property sensitivity analysis are shown in Table 1. The sensitivity of the time-to-failure is given as a percent change in the time-to-failure due to varying the individual thermal properties. The results of the sensitivity analysis show that the thermal inputs, specifically the virgin and bulk conductivity and specific heat capacity, have a significant impact on the time-to-failure prediction. The time-scale of the out-of-plane deflection was also changed, but the shape of the deflection was not affected. The thermal predictions from the model, however, show good agreement with data from the intermediate-scale tests, as shown in Fig. 4. Therefore, it can be assumed that the thermal model inputs are correct and, consequently, insignificant in affecting the predictions. Any differences between the model results and test data were associated with the mechanical properties in the structural portion of the model.

Table 1. Sensitivity of the time-to-failure to varying thermal properties.

Parameter	Percent change in TTF from change in input parameters					
	50 %	75 %	90 %	110 %	125 %	150 %
k_v	33.6	17.8	6.2	-5.4	-12.0	-19.5
k_d	3.3	1.2	0.4	-0.4	-0.8	-1.7
k	60.2	21.2	7.1	-5.8	-12.4	-19.9
C_v	-46.9	-23.2	-9.1	9.1	22.8	45.2
C_d	-0.4	0.0	0.0	0.0	0.4	0.4
C	-46.9	-23.2	-9.1	9.1	22.8	45.6
h	-0.8	-0.4	0.0	0.4	0.4	0.8
h_g	-1.2	-0.8	-0.4	0.4	0.8	1.2

The sensitivity analysis was also performed for the mechanical properties in the structural model. Similar to the analysis performed on the thermal properties, the structural model inputs were varied from their original value. The objective of this analysis was to determine the sensitivity of the magnitude and shape of the predicted out-of-plane deflection to varying the structural model inputs. The cause of the difference between the predicted and observed failure directions, as shown in Fig. 4, was investigated. Additionally, the out-of-plane deflection was investigated to determine its sensitivity to the model inputs when considering the initial deflection towards the heat source. The results for the analysis performed for the previously listed cases are shown in Figs. 6–8.

The sensitivity of the out-of-plane deflection to the in-plane thermal expansion, residual elastic modulus, and vertical temperature profile fitting parameter are shown in Figs. 6, 7, and 8, respectively. Varying the in-plane thermal expansion significantly affects the out-of-plane deflection prediction, as shown in Fig. 6. Sufficiently modifying this property may cause the predicted failure direction to change. This is significant because the failure direction is not predicted correctly for some cases, such as the case shown in Fig. 4. Additionally, in all cases, increasing the in-plane thermal expansion increases the initial deflection to more closely agree with testing. The residual elastic modulus has a significant effect on the predicted failure direction, as shown in Fig. 7. However, the residual elastic modulus appears to have no effect on the initial deflection towards the heat source. The vertical temperature profile fitting parameter does not have a significant impact on the failure direction, as shown in Fig. 8. However, the fitting parameter has a significant effect on the initial deflection. Decreasing the parameter to 0.5 changes the parabolic function such that the temperatures at the edge of the laminate are 50 % of those predicted by the model at the mid-height. The results indicate that increasing the vertical temperature gradient increases the deflection towards the heat source.

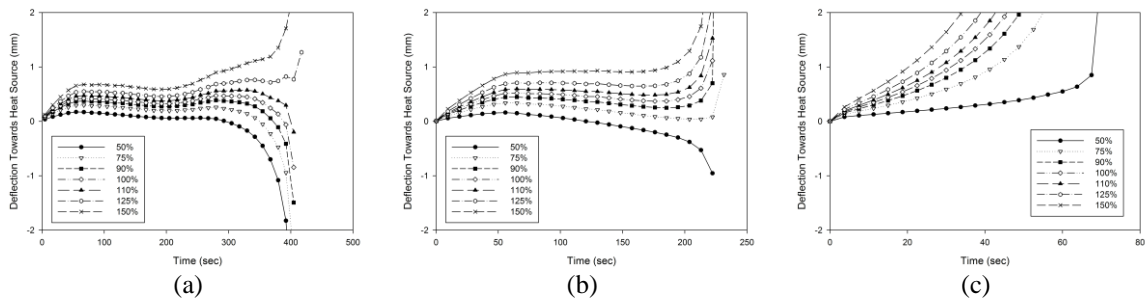


Fig. 6. Sensitivity of out-of-plane deflections to in-plane thermal expansion for the cases of a 12 mm laminate, 38 kW/m^2 heat flux, and loads of: (a) 15 %; (b) 25 %; (c) 50 % of the Euler buckling load.

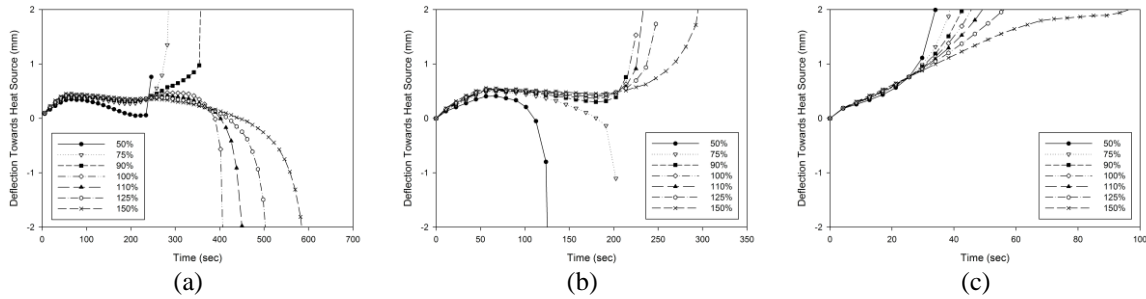


Fig. 7. Sensitivity of out-of-plane deflections to the residual elastic modulus for the cases of a 12 mm laminate, 38 kW/m^2 heat flux, and loads of: (a) 15 %; (b) 25 %; (c) 50 % of the Euler buckling load.

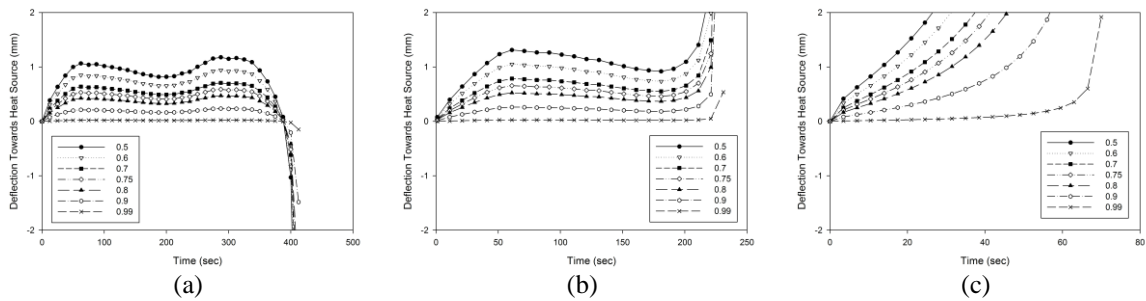


Fig. 8. Sensitivity of out-of-plane deflections to the vertical temperature profile fitting parameter for the cases of a 12 mm laminate, 38 kW/m^2 heat flux, and loads of: (a) 15 %; (b) 25 %; (c) 50 % of the Euler buckling load.

The sensitivity analysis performed for the out-of-plane deflections was also examined to determine the sensitivity of the time-to-failure predictions to the structural model inputs. The objective of this portion of the analysis was to determine the parameters which most significantly affect the time-to-failure predictions. Also, the parameters that were deemed most important were coarsely modified to minimize the difference between the observed and predicted times-to-failure.

Review of the previous analysis for the in-plane thermal expansion in Fig. 6 shows the time-to-failure is not significantly affected by varying this input. Despite having a significant effect on the magnitude and shape of the out-of-plane deflection, this input does not shift the time-scale of failure significantly. The vertical temperature profile fitting parameter in Fig. 7 exhibits similar behavior. However, the residual elastic modulus, shown in Fig. 8, significantly affects both the out-of-plane deflections and time-to-failure predictions. The sensitivity of the time-to-failure predictions to the residual elastic modulus was determined by comparing the predicted and observed times-to-failure for all intermediate-scale tests performed by Summers [21]. The results are similar to that shown in Fig. 5. The metric used to determine the overall effect of varying the residual elastic modulus is the standard deviation of the predicted times-to-failure from those observed in testing. The analysis results are shown in Fig. 9 and Fig. 10 for a 10 % and 25 % reduction in the residual elastic modulus, respectively.

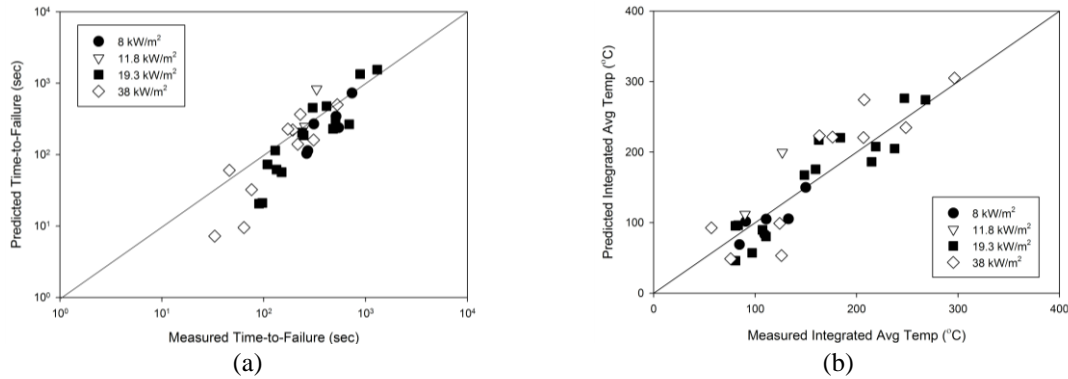


Fig. 9. Sensitivity of the predicted: (a) times-to-failure; (b) average temperatures at failure to reducing the residual elastic modulus by 10 % compared to that observed in testing.

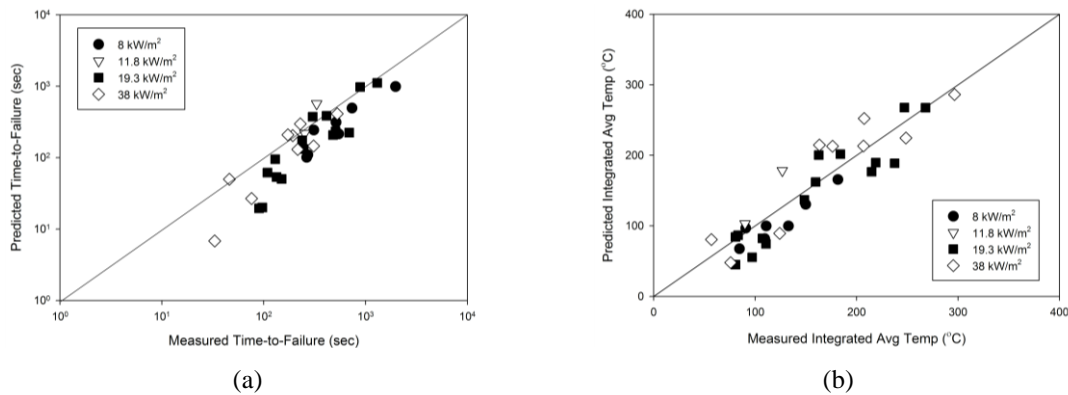


Fig. 10. Sensitivity of the predicted: (a) times-to-failure; (b) average temperatures at failure to reducing the residual elastic modulus by 25 % compared to that observed in testing.

The standard deviation of the predicted times-to-failure from the observed times-to-failure as determined in the thermo-structural model validation in Fig. 5 is 28 %. A 25 % reduction in the residual elastic modulus results in a standard deviation of 24.9 %. This reduction also causes a conservative prediction for a majority of the tests, as shown in Fig. 10. A 10 % reduction in the residual elastic modulus results in a standard deviation of 24.1 %. It is apparent the predicted times-to-failure are sensitive to variations in the residual elastic modulus. The sensitivity analysis demonstrates that the residual elastic modulus used in model

predictions appears to be slightly higher than the ideal value. Therefore, a slight reduction in the residual elastic modulus results in better predictions of the time-to-failure.

CONCLUSIONS

A thermo-structural model was developed to predict the thermal and structural response of compressively loaded FRP laminates in fire conditions. A one-dimensional pyrolysis model was used to predict the temperatures and decomposition state through the laminate thickness. The thermal model was validated using tests performed by Lattimer et al. [20]. The structural model uses an analytical beam model to predict the out-of-plane deflection and failure of compressively loaded laminates exposed to a one-sided heating condition. Intermediate-scale tests performed on E-glass vinyl ester laminates by Summers et al. [24] were used to validate the thermo-structural model.

The validation of the thermo-structural model demonstrated that the model predictions, especially the predicted out-of-plane deflections, are sensitive to the material properties. Therefore, the thermal and mechanical material properties were analyzed to determine their effect on the predicted out-of-plane deflection and time-to-failure. The thermal properties significantly affect the time-to-failure predictions; however, thermal predictions were shown to be in good agreement with measured temperatures in testing. Therefore it is not recommended that these properties be more thoroughly investigated to reconcile differences in the out-of-plane deflections and times-to-failure. The structural properties, specifically the in-plane thermal expansion, residual elastic modulus, and vertical temperature profile fitting parameter, have a significant effect on the out-of-plane deflection predictions. Therefore, accurate knowledge of these parameters is required to predict the deflection response of the laminates. The time-to-failure prediction is only significantly sensitive to the residual elastic modulus. The out-of-plane deflections were also observed to be sensitive to the residual elastic modulus. Therefore, the residual elastic modulus, that is the elastic modulus above the glass transition temperature, should be a priority to obtain accurately in order to obtain accurate model predictions.

REFERENCES

- [1] Egglestone, G. and Turley, D., (1994) Flammability of GRP for use in ship structures, *Fire and Materials* 18(4): 255-260, <http://dx.doi.org/10.1002/fam.810180408>
- [2] Henderson, J.B., Wiebelt, J.A., and Tant, M.R., (1985) A model for the thermal response of polymer composite-materials with experimental-verification, *Journal of Composite Materials* 19(6): 579-595, <http://dx.doi.org/10.1177/002199838501900608>
- [3] Henderson, J.B. and Wiecek, T.E., (1987) A mathematical-model to predict the thermal response of decomposing, expanding polymer composites, *Journal of Composite Materials* 21(4): 373-393, <http://dx.doi.org/10.1177/002199838702100406>
- [4] McManus, H.L.N. and Springer, G.S., (1992) High-temperature thermomechanical behavior of carbon-phenolic and carbon-carbon composites, I. Analysis, *Journal of Composite Materials* 26(2): 206-229, <http://dx.doi.org/10.1177/002199839202600204>
- [5] McManus, H.L.N. and Springer, G.S., (1992) High-temperature thermomechanical behavior of carbon-phenolic and carbon-carbon composites, II. Results, *Journal of Composite Materials* 26(2): 230-255, <http://dx.doi.org/10.1177/002199839202600205>
- [6] Gibson, A.G., Wu, Y.S., Chandler, H.W., Wilcox, J.A.D., and Bettess, P., "A model for the thermal performance of thick composite laminates in hydrocarbon fires," *Revue de L'Institut Francais du Petrol*, 1995, pp. 69-74.
- [7] Bai, Y., Vallee, T., and Keller, T., (2008) Modeling of thermal responses for FRP composites under elevated and high temperatures, *Composites Science and Technology* 68(1): 47-56, <http://dx.doi.org/10.1016/j.compscitech.2007.05.039>
- [8] Sullivan, R.M. and Salamon, N.J., (1992) A finite-element method for the thermochemical decomposition of polymeric materials-I. Theory, *International Journal of Engineering Science* 30(4): 431-441, [http://dx.doi.org/10.1016/0020-7225\(92\)90035-F](http://dx.doi.org/10.1016/0020-7225(92)90035-F)

- [9] Sullivan, R.M. and Salamon, N.J., (1992) A finite-element method for the thermochemical decomposition of polymeric materials-II. Carbon phenolic composites, *International Journal of Engineering Science* 30(7): 939-951, [http://dx.doi.org/10.1016/0020-7225\(92\)90021-8](http://dx.doi.org/10.1016/0020-7225(92)90021-8)
- [10] Milke, J.A. and Vizzini, A.J., (1991) Thermal response of fire-exposed composites, *Journal of Composites Technology and Research* 13(3): 145-151, <http://dx.doi.org/10.1520/CTR10219J>
- [11] Lua, J., O'Brien, J., Key, C.T., Wu, Y., and Lattimer, B.Y., (2006) A temperature and mass dependent thermal model for fire response prediction of marine composites, *Composites Part A: Applied Science and Manufacturing* 37(7): 1024-1039, <http://dx.doi.org/10.1016/j.compositesa.2005.01.034>
- [12] Gibson, A.G., Wu, Y.S., Evans, J.T., and Mouritz, A.P., (2006) Laminate theory analysis of composites under load in fire, *Journal of Composite Materials* 40(7): 639-658, <http://dx.doi.org/10.1177/0021998305055543>
- [13] Feih, S., Mathys, Z., Gibson, A.G., and Mouritz, A.P., (2007) Modelling the compression strength of polymer laminates in fire, *Composites Part A: Applied Science and Manufacturing* 38(11): 2354-2365, <http://dx.doi.org/10.1016/j.compositesa.2007.04.013>
- [14] Feih, S., Mathys, Z., Gibson, A.G., and Mouritz, A.P., (2007) Modelling the tension and compression strengths of polymer laminates in fire, *Composites Science and Technology* 67(3-4): 551-564, <http://dx.doi.org/10.1016/j.compscitech.2006.07.038>
- [15] Gu, P., Dao, M., and Asaro, R.J., (2009) Structural stability of polymer matrix composite panels in fire, *Marine Structures* 22(3): 354-372, <http://dx.doi.org/10.1016/j.marstruc.2009.04.001>
- [16] Asaro, R.J., Lattimer, B., and Ramroth, W., (2009) Structural response of FRP composites during fire, *Composite Structures* 87(4): 382-393, <http://dx.doi.org/10.1016/j.compstruct.2008.02.018>
- [17] Liu, L., Kardomateas, G.A., Birman, V., Holmes, J.W., and Simites, G.J., (2006) Thermal buckling of a heat-exposed, axially restrained composite column, *Composites Part A: Applied Science and Manufacturing* 37(7): 972-980, <http://dx.doi.org/10.1016/j.compositesa.2005.04.006>
- [18] Kardomateas, G.A., Simirses, G.J., and Birman, V., (2009) Structural integrity of composite columns subject to fire, *Journal of Composite Materials* 43(9): 1015-1033, <http://dx.doi.org/10.1177/0021998308097733>
- [19] Liu, L., Holmes, J.W., Kardomateas, G.A., and Birman, V., (2009) Compressive response of composites under combined fire and compression loading, *Fire Technology*, <http://dx.doi.org/10.1007/s10694-009-0123-7>
- [20] Lattimer, B.Y., Ouellette, J., and Trelles, J., (2009) Thermal response of composite materials to elevated temperatures, *Fire Technology*, <http://dx.doi.org/10.1007/s10694-009-0121-9>
- [21] Frangi, A. and Fontana, M., (2003) Charring rates and temperature profiles of wood sections, *Fire and Materials* 27(2): 91-102, <http://dx.doi.org/10.1002/fam.819>
- [22] Mouritz, A.P. and Mathys, Z., (1999) Post-fire mechanical properties of marine polymer composites, *Composite Structures* 47(1-4): 643-653, [http://dx.doi.org/10.1016/S0263-8223\(00\)00043-X](http://dx.doi.org/10.1016/S0263-8223(00)00043-X)
- [23] Goodrich, T.W., Thermophysical properties and microstructural changes of composite materials at elevated temperatures. Master Thesis 2009. Virginia Polytechnic Institute & State University.
- [24] Summers, P.T., Predicting compression failure of fiber-reinforced polymer laminates during fire. Master Thesis 2010. Virginia Polytechnic Institute & State University.